

Quantum Stereodynamics for the Two Product Channels of the F + HD Reaction from the Complete Scattering Matrix in the Stereodirected Representation[†]

D. Skouteris,^{*,‡} D. De Fazio,^{*,§} S. Cavalli,^{*,||} and V. Aquilanti^{||}

Dipartimento di Matematica e Informatica, Università degli Studi di Perugia, 06123 Perugia, Italy, Istituto di Metodologie Inorganiche e dei Plasmi, CNR, 00016 Roma, Italy, and Dipartimento di Chimica, Università degli Studi di Perugia, 06123 Perugia, Italy

Received: May 27, 2009; Revised Manuscript Received: July 30, 2009

For the two exit arrangements of the F + HD reaction, the full scattering matrix is obtained by exact quantum dynamics on an accurate potential energy surface. The **S** matrix is expressed in the stereodirected representation, for the first time, for all channels of a triatomic reaction. We analyze a collision energy where the dominant reaction mechanism is direct and a total angular momentum $J = 0$. It is found that the introduction of steric quantum numbers (correlated in the vector model to the angles measuring directions of approaching reactants and of separating products) provides a sharp description of stereodynamical features for both exit channels.

1. Introduction

The elements of the state-to-state **S** matrix are the most detailed piece of information obtainable from a scattering calculation (with “state” meaning both channel and partial wave). From them, all experimental observables can be obtained. By means of unitary transformations, the **S** matrix can be expressed in a multitude of equivalent representations. Among these, the preferred representations of asymptotic states are those where the particles are characterized by well-defined rotational angular momentum and vibrational quantum numbers (j, v), as well as a definite relative translational energy (E_{tr}). The ones preferentially used and obtained from quantum mechanical calculations are the orbital and the helicity representations.

However, other representations can provide complementary pictures of the scattering event that can lead to an increased understanding of the mechanisms governing elementary molecular collision processes. The use of these alternatives such as our stereodirected representations (SDR)^{1,2} can be of help in elucidating the results of stereodynamic experiments.³ The correlation between attack and recoil angles for the Li + HF reaction has been analyzed using a stereodirected representation,^{4,5} later also applied for the F + H₂ reaction.⁶ More recently, we have focused our attention on the discrete variable representation (DVR) method developed by Light and co-workers.^{7–9} Using this method, we have calculated reaction probabilities for specific attack and recoil angles using a Gauss-Legendre quadrature DVR representation for the angular localization.^{10,11} We have compared the results obtained this way with the corresponding SDR, obtaining further insight in spite of the differences between the two approaches.

In the present paper, the **S** matrix elements obtained for both product channels of the F + HD reaction are transformed into the stereodirected representation and the implications of the results are discussed. Our aim is to evaluate the two basis sets (stereodirected and angular momentum) and their respective capacities to describe the reaction event in a thorough way.

Recent experiments^{12,13} have revealed that this reaction in different energy and angular momentum ranges exhibits pronounced resonance behavior and features of a direct mechanism. These aspects are consistently reproduced by theoretical calculations. The **S** matrix elements needed for our study have been obtained from rigorous time-independent scattering calculations previously published^{14–16} and already used to investigate angular correlation effects. These **S** matrices have been transformed into one of the SDR representations which essentially constitute linear combinations of reactant and product rotational states. We have then calculated reaction probabilities in this alternative representation to work out information regarding the angular dependence of the reaction, and in particular the correlation between the attack and recoil angles of this triatomic system for both exit channels.

For purposes of illustration, here we will consider only scattering at a total angular momentum $J = 0$. We demonstrate that, even with this restriction, the stereodynamic effects are striking enough to merit justification in terms of the potential energy surface and to indicate that, possibly to a smaller degree, the effect would persist at higher partial waves as well.

The organization of the paper is as follows: In section 2, the computational procedure is illustrated, along with the angle-specific representation utilized. In section 3 we give some details of the calculation. In section 4, results are presented and a discussion is made to rationalize the observed trends, and some conclusions are given in section 5.

2. Theory and Computational Procedure

2.1. Stereodirected Representation (SDR). The stereodirected representation of the scattering matrix, developed in our laboratory in the early 90s, provides an analysis of the dynamics of elementary chemical reactions in terms of correlations between attack and recoil angles. The details of the analytical derivation of the equations and their ranges of application have been illustrated in previous papers.^{1,2} In the following, we shortly review those aspects of the theoretical methodology needed for the discussion of the observed pattern.

In the standard SDR representation considered here,^{1,2} the matrix elements connecting it with the j representation are given by the equation (simplified for the $J = 0$ case):

[†] Part of the “Vincenzo Aquilanti Festschrift”.

[‡] Dipartimento di Matematica e Informatica, Università degli Studi di Perugia.

[§] IMIP-CNR.

^{||} Dipartimento di Chimica, Università degli Studi di Perugia.

$$\langle vj|v\nu\rangle = (-1)^{j-\nu+j_{\max}/2} \left\langle \frac{j_{\max}}{2} + \nu, \frac{j_{\max}}{2} - \nu | j0 \right\rangle \quad (1)$$

where the bracket implies a Clebsch–Gordan coefficient and j_{\max} is the maximum value of the rotational quantum number j , accessible at the total energy examined for the vibrational manifold ν under study. As a result, for different vibrational levels, j_{\max} decreases with increasing ν . From this notation we see that $j = 0, \dots, j_{\max}$ and that the relevant ν quantum number takes values

$$\nu = \frac{j_{\max}}{2}, \frac{j_{\max}}{2} - 1, \dots, -\frac{j_{\max}}{2} \quad (2)$$

The values of ν are integral or half-integral, depending on whether j_{\max} is even or odd, respectively.

The characteristic of the SDR which is of interest for our purposes is that, as j_{\max} tends to infinity, SDR wave functions tend to become localized around a specific angle value obeying the equation

$$\cos \theta_\nu = -\frac{2\nu}{j_{\max} + 1} \quad (3)$$

The allowed values of ν select values of θ lying within an angular range that in the semiclassical limit is $-1 + 1/j_{\max} \leq \cos \theta_\nu \leq 1 - 1/j_{\max}$. The intervals close to zero and π , which delimit the classically forbidden region, are excluded. Because of the correspondence given by eq 3, ν can be called steric quantum number. The angle value given by this formula, θ_ν , provides a definition for what is going to be termed henceforth as the *attack/recoil angle* for the SDR representation. Accordingly, the specific θ_ν that we will encounter below will be denoted as ϕ , δ , or η . It should be kept in mind that for relatively small j_{\max} (as would be, for example, the case for light molecules such as H_2) the angle localization of the SDR wave function becomes less sharply defined, especially for near-collinear configurations.¹⁷

In this work we consider all three channels of the $\text{F} + \text{HD}$ reaction and we have found it convenient to label the respective Jacobi angles as shown in Figure 1.

2.2. S Matrix Transformation. Briefly, the **S** matrix elements are obtained as sketched in section 3. Once the **S** matrix is obtained in this way, it is expressed in what was termed before as the νj representation. It is transformed to an alternative representation using the standard technique of matrix transformation, inserting two complete sets into the matrix element of the **S** operator:

$$\langle \nu' \nu' | \hat{S} | \nu \nu \rangle = \sum_{j j'} \langle \nu' \nu' | \nu' j' \rangle \langle \nu' j' | \hat{S} | \nu j \rangle \langle \nu j | \nu \nu \rangle \quad (4)$$

Here ν denotes a generic quantum number but the idea is that, as opposed to the νj representation, the $\nu \nu$ wave functions should be localized as much as possible around certain angles. In this way, the transformed **S** matrix elements provide us with information regarding angular selectivity and specificity of the reaction under consideration. The angles mentioned here are termed as the *attack and recoil* angles for the reactant and product arrangements, respectively, and are defined (for a generic $A + BC$ system) as the angle between the interatomic

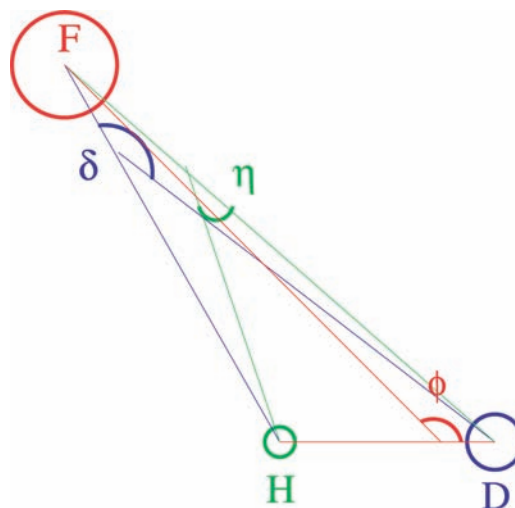


Figure 1. Schematic view of angles between Jacobi vectors for the three arrangements of the FHD system at the transition state. The relative masses are changed at 5, 2, and 1 for the F, D, and H atoms, respectively, for ease of illustration. In this paper, ϕ is the attack angle by F on HD and η and δ are those for the recoil of H and D, respectively.

vector of the diatomic unit (the BC vector) and the vector pointing from the center of mass of the diatomic toward the atom (the $A - BC$ vector) as shown in Figure 1. Being essentially latitude angles, both attack and recoil angles range between 0 and 180°.

Obviously, the $\nu \nu$ representation being as discrete as the νj representation, some degree of angular delocalization is always to be expected. The uncertainty principle between angle and angular momentum is a limit to the angular resolution obtainable (see ref 18 for a recent discussion). The more the angle is to be localized, the larger is the number of j states that have to be included in the set. Conversely, the better defined j is, the more the angle-localized wave function is going to be diffused. In our angle-localized basis set, the maximum j (j_{\max}) we are using must be included as an additional ingredient, as the resulting angle-localized wave function will certainly depend on its value.

Another limit is imposed by energy conservation. If the total energy of our reactant or product state is known and fixed, the number of diatomic j states we can coherently combine is obviously bounded by energetic considerations. Hence, low total energy necessarily implies a low angular resolution.

There is one more specific feature to be considered. Since the angle-localized wave functions result from the coherent superposition of wave functions with a definite j and total energy, it implies that the *translational* part of the wave function will be different for each j state. In other words, an angle-specific wave function at a fixed total energy will have the form

$$|v\nu\rangle = \sum_j c_j |v j\rangle e^{-ikR} \quad (5)$$

$$k^2 = 2\mu(E_{\text{tot}} - E_{v_j}) \quad (6)$$

where R is the length of the Jacobi vector defined above (see Figure 1), c_j are the coefficients determined in eq 1, and μ is the two bodies (atom–diatom) reduced mass of the arrangement under study. From the j -dependence of k , it is obvious that each j state will be included in the sum with its own phase factor, which will depend on R . If, instead, one attempts to fix the

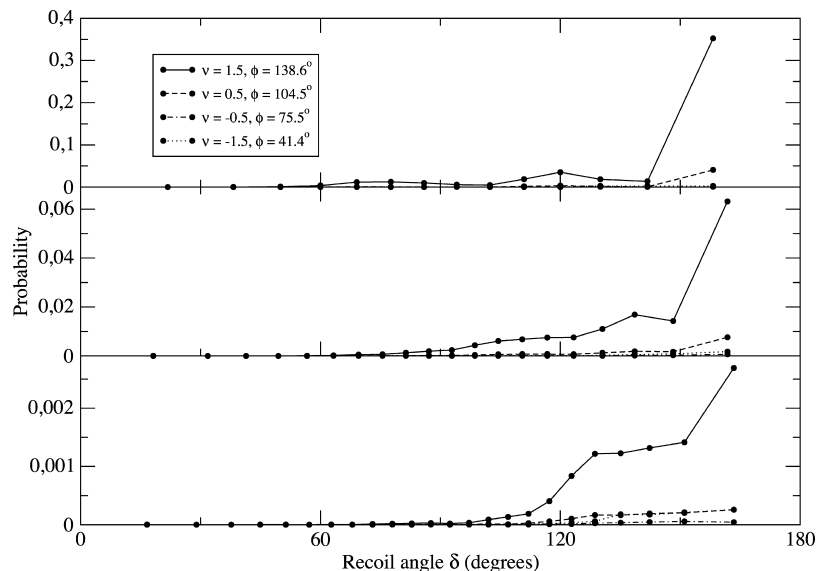


Figure 2. Reaction probability with respect to recoil angles for the HF + D channel, for product vibrational quantum numbers $v' = 0$ (lower panel, $j'_{\max} = 23$), $v' = 1$ (middle panel, $j'_{\max} = 19$), and $v' = 2$ (upper panel, $j'_{\max} = 13$). Here, the data for $\phi = 104.5^\circ$ and especially $\phi = 138.6^\circ$ are so small as to be hardly distinguishable from zero.

translational instead of the *total* energy, each j state will correspond to a different total energy, and what is now a phase depending on distance will be then a phase depending on *time* because the time-dependent phase factor depends on the total energy. Either way, the angular orientation of our wave function is not permanent, as a result of its spatial or temporal distortion. As a result, the angle around which our wave function is localized has a narrow spread in the neighborhood of $R = 0$, i.e., when the atom is approaching the center of mass of the diatom and therefore all phase factors e^{-ikR} are equal to 1.

Thus, the terms *attack angle* and *recoil angle* are understood to mean the angles as defined before, but the wave functions themselves strictly refer to these angles when the atom is very close to the center of mass of the diatomic (in either the reactant or product arrangements). Each possible representation is essentially defined by its set of matrix elements $\langle \nu\nu' | \nu j \rangle$ as shown in eq 1, where $|\nu j\rangle$ is a ket in the νj representation and $|\nu\nu'\rangle$ is a ket in the angle-localized representation.

3. Details of the Calculation

The **S** matrix data used here were obtained by an exact method as described in our previous work on the F + H₂^{19–24} and in particular on the F + HD^{14–16} reactions. The potential energy surface is the one denoted as PES-III²⁰ in these references, tested against experimental data and specifically against isotopic branching ratios. The computer code provides the full scattering matrix in the helicity representation. In this representation, the labels for reactant and product channels are the vibrational and the rotational angular momentum quantum numbers of the molecule, and the helicity quantum number, Ω . The latter is the projection that both total and rotational angular momentum quantum numbers make about the relative velocity vector. In the case of $J = 0$ scattering, Ω is zero as well and the reactant and product quantum states are simply labeled as $|\nu j\rangle$ and $|\nu' j'\rangle$, respectively.

In the case illustrated here, we consider both product channels of the F + HD($v=0, j$) reaction at $J = 0$ and for a total energy $E_{\text{tot}} = 1.667$ eV (with the zero fixed at the bottom of the product well), corresponding to a collision energy of 76.0 meV. The accessible values for j are 0, 1, 2, and 3 so that $j_{\max} = 3$. This

energy corresponds, for $J = 0$, to a position just outside the long-lived resonance region studied in ref 15 and hence the “classical” behavior of the system is expected to predominate.

4. Results

In Figures 2–4 results are shown for both the HF + D and DF + H channels at a total angular momentum $J = 0$. In each figure, the reaction probability is plotted against the corresponding recoil angles δ and η (in degrees). In each graph four curves are shown, each one corresponding (as described in the legends) to a specific entrance stereodirected quantum number ν . Note that the attack angle ϕ given in the captions does not contain a sharp indication on directional properties since there are only four rotational states of the HD molecule open at this energy and the corresponding stereodirected wave function is rather delocalized. Nevertheless, as will be shown in the next subsections, the representation provides important information on the reaction mechanism by distinguishing the attack of the fluorine atom from the hydrogen or the deuterium side and/or from insertion attack between them. On the other hand, there is a large number of rotational states available to the products (35 in the case of the ground vibrational state of DF) and thus the concept of the exit angles δ and η , being directly correlated to the exit quantum number ν' , is accordingly much sharper.

4.1. HF + D Channel. In all three curves pertaining to the HF + D channel (shown in Figure 2), the reaction probability is concentrated around large recoil angles δ . Moreover, for all three open vibrational quantum numbers of the HF product, there is substantial stereoselectivity with respect to the entrance ν quantum number with the maximum reaction probability at $\nu = 1.5$ in all cases. In fact, typically, the overall reaction probability of the other stereodirected states is less than 10% of the whole. Even though there is substantial delocalization of the reactivity with respect to the exit angles, the maximum always occurs at the exit angle δ near 180° , that is, at the configuration closest to collinearity. At the opposite half of the exit sphere, the reaction probability is essentially zero. One can infer, on classical grounds, that the 180° configuration is the one corresponding to a collinear FH–D arrangement (confirmed also by Figure 1). This picture is also borne out by the fact that

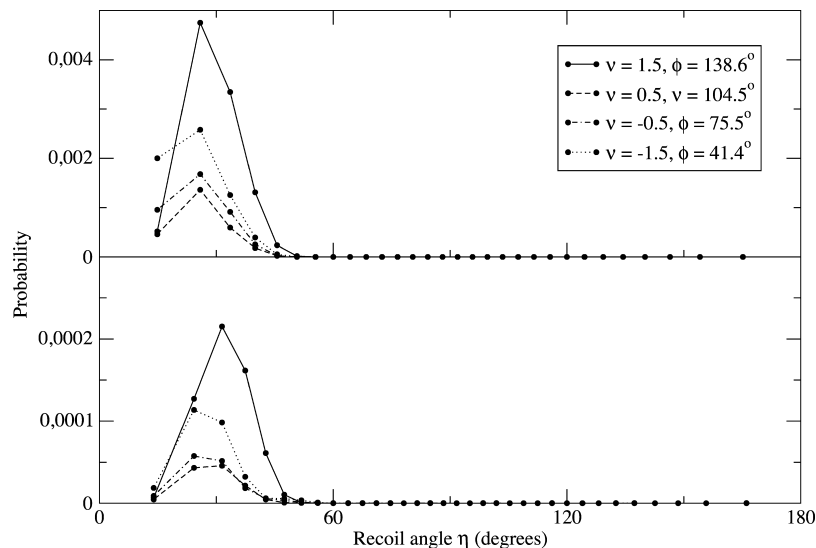


Figure 3. As in Figure 1, for the DF + H channel and for product vibrational quantum numbers $v' = 0$ (lower panel, $j'_{\max} = 33$) and $v' = 1$ (upper panel, $j'_{\max} = 29$).

the angular localization of the stereodirected states is maximum for small values of the R product Jacobi coordinate, i.e., when the D unit has not had time to move away from HF and HF has not had time to rotate.

At $v' = 0$ the values of the reaction probabilities are small. As v' increases, so do the reaction probabilities and so does the product angle stereospecificity. The effect becomes rather dramatic at $v' = 2$. Here, even though there are 14 open rotational states of HF, around 20% of the total reactivity is concentrated on one exit number v' only. This provides a striking illustration of the compression of information provided by switching to the stereodirected representation from the standard j one.

To extract information on the reaction mechanism, we must take into account that, in the limit of a sudden model for a direct reaction, the new bond is formed at the same time that the old one is broken, so that attack and recoil angles should both reflect the same internuclear geometry where the reaction occurs. For the HF + D product channel both the attack and the recoil probabilities have a maximum at the extremes of the angular ranges of the permitted values, showing a sharp tendency to favor the reaction when the fluorine atom is attacking from the hydrogen end. This attack should also be favored by the screening effect of the hydrogen atom due to the asymmetry of the rotations of the HD molecule.^{25,26} In ref 16, from an analysis of the reactive state-to-state integral cross sections, we have shown for this channel the presence of two different direct mechanisms, one prevalent at low collision energies (<40 meV) and the other arising above 40 meV and rapidly increasing with energy. In the first mechanism, dominated by tunneling, the fluorine atom overcomes the transition state with the bent geometry of Figure 1 whereas in the second case the crossing takes place predominantly in a collinear configuration. From Figure 2 we can observe that the high delocalization of the stereodirected wave function due to the low number of the open rotational states does not permit us to discriminate between the two direct mechanisms. In fact, the attack and the recoil angles (see Figure 1) at the transition state with the F atom approaching from the H side, are 132 and 160°, in the neighborhood of the last allowed values of the ϕ and δ angular ranges. In view of the relatively high collision energy examined here, we expect that most of the reactivity of this channel is due to a collinear

approach. Whether other minor maxima at smaller recoil angles are due to residues of resonance effects should be ascertained by further stereodynamical studies in a larger range of energies.

4.2. DF + H Channel. The results pertaining to the DF + H channel are shown in Figures 3 and 4. Because of the smaller vibrational frequency of DF, there are four vibrational states of DF open at this energy. Moreover, since the rotational constant of DF is smaller than the one of HF, the number of available rotational (and hence also stereodirected) states at each vibrational level is higher. We are therefore in a better condition to extract information on the reaction mechanism because the delocalization of the stereodirected wave functions is lower. The lowest recoil angle η ranges, in this case, from about 14° at $v' = 0$ to about 19° at $v' = 3$.

For all four vibrational states, the reaction probability is concentrated around a single maximum at low recoil angles. As in the case of HF + D, there is substantial stereoselectivity with respect to the reactant state but to a smaller degree. In fact, here we can observe a new behavior not present in the HF + D case: the dominant reactant v quantum number is 1.5 for the $v' = 0$ product state, but this changes smoothly to -1.5 going toward $v' = 3$, whereas the more “perpendicular” attack quantum numbers are the least reactive ones.

The results shown here can be explained in the framework described in the previous subsection. The larger number of stereodirected states available permits us to distinguish better the bent structure of the transition states especially for low vibrational quantum number where the localization of the stereodirected wave function is higher. However, in the DF + H case both transition states can be crossed and the relevance of the two reaction mechanisms is strongly dependent on the vibrational quantum number. The relevance of the attack from the H side for the DF + H reaction and its sensitivity to the vibrational quantum numbers of the product, has already been discussed in the literature. Aoiz et al.²⁷ have found this effect in quasi-classical trajectories calculations and termed it “migratory trajectories”, and experimental evidence has also been reported in ref 12. The physical explanation can be given by the features of the potential energy surface and in particular by the orientation properties of the perpendicular van der Waals well entrance channel. Because of this interaction, the HD molecule can change its orientation when the fluorine atom is

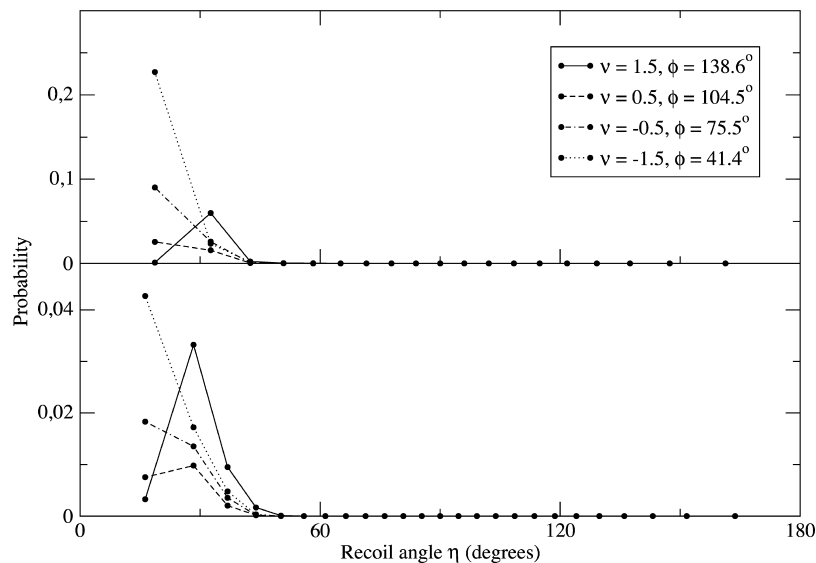


Figure 4. As in Figure 1, for the DF + H channel and for product vibrational quantum numbers $\nu' = 2$ (lower panel, $j'_{\max} = 24$) and $\nu' = 3$ (upper panel, $j'_{\max} = 18$).

approaching so that atoms initially attacking the H end of the diatom are pulled toward the D side. When the incoming atom attacks the D end, the orientation effect is lower because of the lower angular anisotropy (see Figure 15 of ref 27), a mechanism not active for the HF + D channel. The larger capability of the van der Waals forces to influence the attack angle when the incoming atom comes from the H side, was also found in ref 28 for the Cl + HD reaction, although, in that case, the orientation effect suppressed reactivity because of the collinear geometry of the transition state. We can note that the potential energy surface used in our work (the PES-III) has the entrance channel van der Waals well significantly shallower²⁰ than in the SW PES,²⁹ used in ref 27. However, in our case the well extends at larger interatomic distances so that the angular forces can act in a wider range. For this reason, stereodynamic effects can be stronger in PES-III¹⁴ in spite of the smaller depth of the well.

More results can be explained in this frame. The acceptance cone²⁵ is slightly larger (by about 7° at the transition state geometry; see Figure 1) when the fluorine atom approaches from the D end, so that the probabilities for $\nu = -0.5$ are always larger than the ones for $\nu = 0.5$. A general tendency to shift the probability distributions at larger recoil angles for positive ν , especially for higher vibrational quantum numbers (Figure 4), can be noted, a possible quantum manifestation of the classical migratory mechanism that favors naturally a bent approach and that the η angle at the transition state geometry is slightly larger when the fluorine atom approaches from the H end (see Figure 1).

Because of the higher number of open rotational states, the compression effect seen in HF + D is even more prominent here. In all cases, the reactivity is concentrated into about 5 stereodirected product states. Comparing this number to the 35 open rotational states for $\nu' = 0$ or the 20 rotational states for $\nu' = 3$ (where the reactivity is confined to 3 product states), one can see that the stereodirected basis constitutes an excellent tool for compressing scattering information for this reaction.

5. Conclusions and Future Work

The stereodynamics of the F + HD reaction has been studied in the stereodirected representation, for the $J = 0$ partial wave at an energy where resonance effects (if present) are expected

to be small with respect to a dominating direct mechanism. In both HF + D and DF + H channels there is a clear bias for the reaction probability in the stereodirected representation toward one or the other of the collinear ends of the angular range. The effect is particularly sharp for the more “classical” DF + H channel, where the stereodirected representation of the **S** matrix results in a considerable condensation of information.

Notwithstanding the unavoidable limitations imposed by the uncertainty principle,¹⁸ much information on the reaction mechanisms can be extracted. In particular, there is a clear propensity for the HF + D reaction to react exclusively when the incoming F atom attacks from the H end whereas attack from both ends can lead to reaction for DF + H. Although the higher wave function delocalization in the HF + D case does not give a clear picture for this channel, we can observe an evident propensity for DF + H to react via a more “classical” behavior, following the minimum energy path and by crossing the transition state in its bent configuration. Otherwise, a near collinear crossing is preferred for HF + D.¹⁶ The key features of the potential responsible for such different dynamics between the two reactions is the entrance channel van der Waals well that can efficiently address fluorine atoms initially attacking from the hydrogen end to react with the deuterium atom. From this point of view, this work can be considered another piece of evidence for how small interactions, such as van der Waals forces, can strongly influence reaction dynamics.

Since the complete **S** matrix for the system is available, this approach can be extended to higher partial waves and other energy values. Moreover, the stereodirected transformation reported in this work is quite general and can be also applied to the **Q** matrix of the system, also available,¹⁵ to study the delay time of a particular stereodirected state, increasing our capability to obtain a physical understanding of the reaction mechanisms. It will be particularly interesting to carry out work with the aim to elucidate the influence of resonances on the stereodynamics of the reaction.

Acknowledgment. V.A. and S.C. acknowledge the Italian Space Agency (ASI) for funding and MIUR for a PRIN contract. D.D.F. also wants to thank his institution (CNR) for the award of a research financing by RSTL.

References and Notes

- (1) Aquilanti, V.; Cavalli, S.; Grossi, G.; Anderson, R. W. *J. Phys. Chem.* **1991**, *95*, 8184.
- (2) Anderson, R. W.; Aquilanti, V.; Cavalli, S.; Grossi, G. *J. Phys. Chem.* **1993**, *97*, 2443.
- (3) See recent thematic issues on chemical stereodynamics: *Chem. Phys.* **2004**, *301*, 159–334. and *Eur. Phys. J. D* **2006**, *38* 1–236.
- (4) Alvarino, J. M.; Aquilanti, V.; Cavalli, S.; Crocchianti, S.; Laganà, A.; Martinez, T. *J. Chem. Phys.* **1997**, *107*, 3339.
- (5) Alvarino, J. M.; Aquilanti, V.; Cavalli, S.; Crocchianti, S.; Laganà, A.; Martinez, T. *J. Phys. Chem.* **1998**, *102*, 9638.
- (6) Aldegunde, J.; Alvarino, J. M.; De Fazio, D.; Cavalli, S.; Grossi, G.; Aquilanti, V. *Chem. Phys.* **2004**, *301*, 251.
- (7) Lill, J. V.; Parker, G. A.; Light, J. C. *Chem. Phys. Lett.* **1982**, *89*, 483.
- (8) Light, J. C.; Hamilton, I. P.; Lill, J. V. *J. Chem. Phys.* **1985**, *82*, 1400.
- (9) Bacić, Z.; Light, J. C. *Annu. Rev. Phys. Chem.* **1989**, *40*, 469.
- (10) Skouteris, D.; Laganà, A. *J. Phys. Chem. A* **2006**, *110*, 5289.
- (11) Skouteris, D.; Crocchianti, S.; Laganà, A. *Chem. Phys. Lett.* **2007**, *440*, 1.
- (12) Dong, F.; Lee, S.-H.; Liu, K. *J. Chem. Phys.* **2006**, *124*, 224312.
- (13) Lee, S.-H.; Dong, F.; Liu, K. *J. Chem. Phys.* **2006**, *125*, 133106.
- (14) De Fazio, D.; Aquilanti, V.; Cavalli, S.; Aguilar, A.; Lucas, J. M. *J. Chem. Phys.* **2006**, *125*, 133109.
- (15) De Fazio, D.; Cavalli, S.; Aquilanti, V.; Buchachenko, A.; Tschberbul, T. V. *J. Phys. Chem. A* **2007**, *111*, 12538.
- (16) De Fazio, D.; Aquilanti, V.; Cavalli, S.; Aguilar, A.; Lucas, J. M. *J. Chem. Phys.* **2008**, *129*, 064303.
- (17) de Miranda, M. P.; Crocchianti, S.; Laganà, A. *J. Phys. Chem. A* **1999**, *103*, 10776.
- (18) Anderson, R. W.; Aquilanti, V. *J. Chem. Phys.* **2006**, *124*, 214104.
- (19) Aquilanti, V.; Cavalli, S.; Simoni, A.; Aguilar, A.; Lucas, J. M.; De Fazio, D. *J. Chem. Phys.* **2004**, *121*, 11675.
- (20) Aquilanti, V.; Cavalli, S.; De Fazio, D.; Volpi, A.; Aguilar, A.; Lucas, J. M. *Chem. Phys.* **2005**, *308*, 237.
- (21) Aquilanti, V.; Cavalli, S.; De Fazio, D.; Simoni, A.; Tschberbul, T. V. *J. Chem. Phys.* **2005**, *123*, 054314.
- (22) Sokolovski, D.; Sen, S. K.; Aquilanti, V.; Cavalli, S.; De Fazio, D. *J. Chem. Phys.* **2007**, *126*, 084305.
- (23) Sokolovski, D.; De Fazio, D.; Cavalli, S.; Aquilanti, V. *J. Chem. Phys.* **2007**, *126*, 121101.
- (24) Sokolovski, D.; De Fazio, D.; Cavalli, S.; Aquilanti, V. *Phys. Chem. Chem. Phys.* **2007**, *9*, 5664.
- (25) Johnston, G. W.; Kornweitz, H.; Schechter, I.; Persky, A.; Bersohn, R.; Levine, R. D. *J. Chem. Phys.* **1991**, *94*, 2749.
- (26) Manolopoulos, D. E. *J. Chem. Soc., Faraday Trans.* **1997**, *93*, 673.
- (27) Aoiz, F. J.; Bañares, L.; Herrero, V. J.; Saez Rabanos, V.; Stark, K.; Werner, H.-J. *J. Chem. Phys.* **1995**, *102*, 9248.
- (28) Skouteris, D.; Manolopoulos, D.; Bian, W.; Werner, H.-J.; Lay, L.-H.; Liu, K. *Science* **1999**, *286*, 1713.
- (29) Stark, K.; Werner, H.-J. *J. Chem. Phys.* **1996**, *104*, 6515.

JP904972N